Transmission Electron Microscopy of Ultraprecision and Precision Al-Mg Alloy Machined Surface

Toshiaki KANEEDA*, Seiichi Yokomizo, Kousuke MORIMOTO*, and Ichizo TSUKUDA*****

* :Department of Mechanical Engineering, Okayama University of Science
1-1 Ridai-cho, Okayama, 700-0005 JAPAN
** :Industrial Technology Center of Okayama Prefecture
5301 Haga, Okayama, 701-1296 JAPAN
*** :Showa Aluminum Co.Ltd.
6-224 Kaisan-cho, Sakai-city, Osaka, 590-8576 JAPAN

ABSTRACT Internal microstructure of ultraprecision and precision machined surface have been critically examined with an transmission electron microscope(TEM). TEM observations were carried out on the machined surface layer of Al-Mg alloy from metal physical view point. Ultraprecision machined surface had much more sophisticated values than the precision machined surface in the surface roughness;however, with respect to the dislocation structure, representing as tangled network, of the machined surface, no obvious differences between them could be recognized at all. The observation results provided three types of tangled dislocation network in all cutting conditions. Depth of cut and cutting speed effects on the dislocation network of the ultraprecision machined surface could not be found in all cutting condition.

Key words: *machined surface, microstructure, ultraprecision cutting, transmission electron microscope, dislocation network*

1. INTRODUCTION

Examination of machined surface is usually divided into two groups. One is external characteristics represented as surface roughness, waviness, and so on. The other one is invisible characteristics, that is deformed layer, residual stress, hardness, etc. Precision cutting has recently become a part of conventional manufacturing process. Moreover, ultraprecision cutting could have been accepting as a kind of conventional precision machining. The examinations mentioned above are not sufficiently effective for ultraprecision machined surface in order to inspect the surface property microscopically. Thereby, internal microstructure of ultraprecision machined surface should be critically examined with an appropriate examination. Kaneeda et al. has already revealed microstructure of machined surface[1], chip, shear plane and splitting point [2] in pure aluminum workmaterial, however that was for conventional machining. This study actually focuses ultraprecision and precision cutting.

This paper deals with microstructure, in particular dislocated internal structure, of ultraprecision and precision machined surface layer using a high accelerating voltage, 200kV transmission electron microscope (TEM). Depth of cut and cutting speed effects have been investigated. Differences in the internal structure between ultraprecision and precision cutting were analyzed.

2. EXPERIMENTAL PROCEDURE

2.1 Precision cutting experiments

Precision cutting experiments were conducted on a NC precision cutting apparatus. The apparatus was designed to orthogonal-cut the workmaterial plate having less than 340 mm length at constant cutting speeds up to 50m/min. The apparatus also allows the tool to be held with high rigidity and exact setting depth of cut. Minimum depth of cut is 1μm.

Al-Mg alloy, mentioned after, was used as the workmaterial. The workmaterial having dimensions 150 × 35 × 3 mm were carefully machined in order to obtain uniform depth of cut in the cutting experiments.

Diamond tools had 0° rake angle and 10° clearance angle with a straight edge.

Pre-cutting process should not produce large deformed layer of the machined surface, therefore 1μm depth of cut was selected for precision cutting experiments as a cutting condition.

Table 1 shows the precision cutting conditions. The cutting speed was a constant 25.7m/min. The depth of cut was 1 and 3 μm, which were typical cutting conditions. White kerosene was used as a cutting fluid.

2.2 Ultraprecision cutting experiments

Ultraprecision cutting experiments were conducted on a Rank Pneumo Nanoform 600 to obtain such ultra smooth mirror surfaces as polygon mirrors. The Al-Mg alloy bar having a 65mm diameter for polygon mirrors was used as the workmaterial.

Diamond tools had 0° rake angle and 10° clearance angle with a nose radius of 1mm.

Table 1 Cutting conditions

Cutting form			Ultraprecision cutting (Surfacing)	Precision cutting (Orthogonal)
Workmaterial			Al-Mg Alloy (G56)	
Dimensions of work		mm	ϕ65×15	150×35×3
Tool			Single point diamond tool	Straight edge diamond tool
Tool angle	Rake angle	α °	0	0
	Relief angle	ε °	10	10
Nose radius		mm	1	——
Cutting speeds		m/min	47.1⇔282.6	25.7
Feed rate		μm/rev	8	——
Depth of cut t_1		μm	2, 4 & 8	1, 3
Cutting fluid			White kerosene (Mist type)	White kerosene

Table 2 Chemical composition of Al-Mg alloy

wt %

Purity	Additive elements		Impurities		
	Mg	Cr	Si	Fe	bal
More than 99.99	4.7	0.03	0.003	0.005	0.003

Table 3 Mechanical Properties of Al-Mg alloy

Tensile strength (MPa)	Proof stress (MPa)	Elongation (%)	Microvickers hardness
243	116	46	60

Main spindle turning speed was a constant 2000rpm, so the cutting speeds ranged from 0m/min up to 408.2m/min. Feed rate was 2μm/rev. White kerosene was used as a cutting fluid and supplied to the cutting edge as a mist. Table1 also shows the ultraprecision cutting conditions.

2.3 Workmaterial

Table 2 shows chemical composition of the Al-Mg alloy. The alloy contains 4.1%-Mg to strengthen mechanical properties to avoid such decrease in accuracy of geometry as deflection due to the residual stress: to refine the grain level, obtaining smoother machined surfaces without steps between crystal, namely grain boundary steps.

Before the cutting experiments, 2hour-553K-annealing was carried out to remove the work hardened layer. Table 3 shows mechanical properties of the Al-Mg alloy.

2.4 Specimen preparation for TEM observation

It is very important to obtain thin films without any damage during processing. First, the workmaterial was sliced with less than 0.2mm thickness, by an electric discharge machine with a wire cutting device, along the cutting direction. The thin plate was then electrochemical-jet-polished by a Tenupole-3 (Storeurs Co.) to make a concave lens-shaped thin film. Less than 1 μm thickness Al film can be penetrated by an electron beam with 200 kV accelerating voltage.

3. MACHINED SURFACE PROPERTIES

Table 4 shows the machined surface properties. The surface profiles were measured using a non-contact three dimensional microsurface texture analyzer (Zygo Co). The results establish that ultraprecision cutting provided the ultra smooth surfaces, as might be expected, much more than the precision cutting. The surface profile apparently presented grain boundary steps.

The hardness of the machined surface was measured using a conventional microvickers hardness testing machine with a 25 g load. The hardness in the ultraprecision cutting was much lower than in the precision cutting, being nearly the same as the bulk material. It must be noted that microvickers hardness value offers hardness of region being ten times as deep as indented.

Table 4 Machined surface properties

		Ultraprecision cutting			Precision cutting	
		Al-Mg Alloy (G56)				
Depth of cut t_1 μm		t_1 =2μm	t_1 =4μm	t_1 =8μm	t_1 =1μm	t_1 =3μm
Microvickers hardness Hv		59.5	59.6	58.3	62.6	71.8
Surface roughness	Rmax nm	27.4	20.3	16.9	173.2	318.8
	rms nm	2.7	2.5	2.4	22.9	45.7
	Ra nm	2.1	2.1	1.9	18.6	36.6

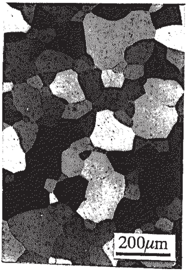

(1) t_1=2μm, V=70.0m/min

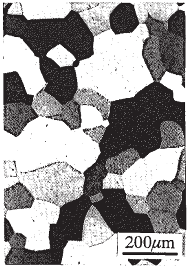

(2) t_1=8μm, V=260.0m/min

Fig.1 Polarizing microscope photo of ultraprecision machined surface

However, it seems reasonable to suppose that the ultraprecision machined surface has much less work-hardened condition than the precision machining and a remarkably thin work-hardened layer.

4. OBSERVATION RESULTS

4.1 Polarizing microscope observation

Fig.1 shows polarizing microscope photos of the ultraprecision machined surface etched by Barker etching solution. Depth of cut t_1 are 2 and 8 μm. The average grain size in Fig.1 was assessed at 68 μm, being identical to the bulk material. The average grain size were the same in all ultraprecision cutting condition. In other words, depth of cut and cutting speed effects were not presented.

4.2 Precision machined surface of TEM observation

Fig.2 shows TEM photos of surface microstructure precision machined with depth of cut t_1=3μm. The precision machined surfaces presented three types of dislocation structure. Fig.2 shows two of

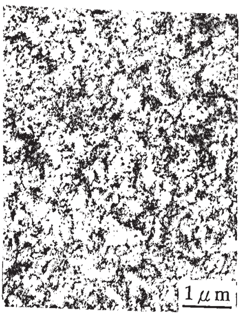

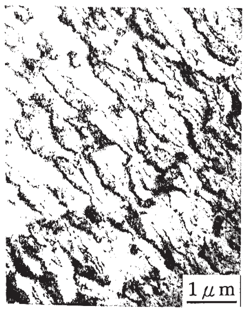

Fig.2 TEM photo of precision machined surface microstructure (t_1=3μm,V=25.7m/min)

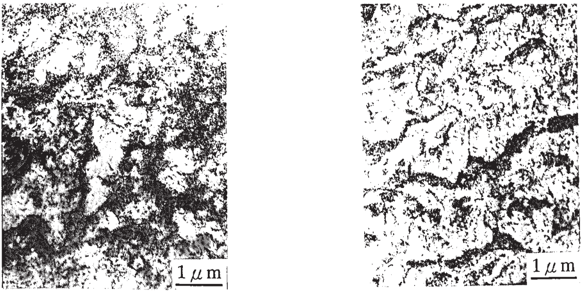

Fig.3 TEM photo of ultraprecision machined surface microstructure (t_1=2 μm, V= 376,8, 62.8m/min)

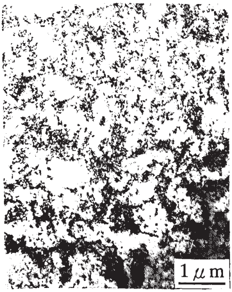

(1) V=251.2m/min

(2) V=376.8m/min

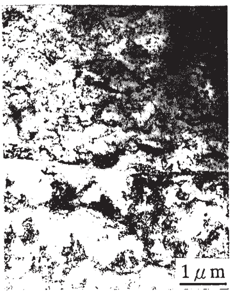

(3) V=125.6m/min

Fig.4 Ultraprecision machined surface microstructure (t_1=8 μm)

them: one was a tangled dislocation network, and the other one was an elongated cell structure being similar to a chain of islands. The crystallographic orientation appears to control the type of dislocation distribution. The last type was shown in Fig.4(2). This is somewhat uniform tangled-dislocation distribution.

As the plastic deformation increases in the primary deformation zone of the workmaterial, dislocations remarkably multiplied by frequent cross slip that easily occurs in deformation of high-stacking fault energy-fcc metals like Al, Cu, etc. Subsequently to the multiplications, the dislocations tangled to a great extent and formed cell structure. [3]

4.3 Ultraprecision machined surface of TEM observation

Fig.3 shows TEM photos of surface microstructure ultraprecision machined with depth of cut t_1 $=2\mu m$. No significant differences between the ultraprecision and the precision machined surface in the dislocation distribution could be recognized. That is to say, the three types of dislocation network could be seen as well. It follows from what have been observed that there are not much differences between them on the crystallographic deformation level, namely dislocation theory.

4.4 Depth of cut and cutting speed effects on surface microstructure

Fig. 4 shows TEM photo of surface microstructure ultraprecision machined with depth of cut t_1 $=8\mu m$. The microstructure also provided three types of dislocation network. No obvious differences between depth of cut $t_1=2\mu m$ and $t_1=8\mu m$ in the microstructure could be seen at any cutting speeds.

In addition, no cutting speed effects could not be observed as shown in Fig.1-Fig.4.

5. DISCUSSION

All these things make it clear that the ultraprecision machined surface had much more sophisticated values than the precision machined surface in the surface roughness;however, with regard to the dislocation structure, representing as a tangled network, of the machined surface, no obvious differences between them could not be recognized at all. The microvickers hardness of ultraprecision machined surface indicates that the ultraprecision cutting is capable producing a less work-hardened surface and an remarkably thin work-hardened layer. Based on the analysis mentioned above, it seems reasonable to suppose that the ultraprecision cutting is one of the most mild removal process.

6. CONCLUSIONS

(1) Ultraprecision machined surface has the remarkably smooth surface with less than Ra=2.1nm and nearly the same microvickers hardness as the bulk material.

(2) Precision machined surface has the smooth surface with less than Ra=36.6nm and greater microvickers hardness than the ultraprecision machined surface and the bulk material.

(3) Polarizing microscope observation offered that the average grain size of the crystal in the ultraprecision machined surface was assessed at $68\mu m$, being identical to bulk material.

(4) TEM observation results provided the three types of tangled dislocation network on the machined surfaces in all cutting conditions.

(5) Depth of cut and cutting speed effects on the dislocation network of the ultraprecision machined surface could not be found in all cutting condition.

REFERENCES

[1] T. Kaneeda, S. Yokomizo and D. Higashi: Proc. of the American Soc. of Prec. Eng., 11(1996)176.
[2] T. Kaneeda, H. Kawabe, N. Ikawa and H. Tsuwa: Bull. of the Japan Soc. Prec. Eng., 17, 1(1983)25.
[3] Japan Soc. of Metal ed.: Dislocation Theory (in Japanese), Maruzen(1971) 81.